Available online at www.sciencedirect.com
SCIENCE DIRECT®
International Journal of Heat and Mass Transfer 48 (2005) 2540–2547
International Journal of HEAT and MASS TRANSFER
www.elsevier.com/locate/ijhmt

Determination of liquid–solid mass transfer coefficients for a spinning disc reactor using a limiting current technique

J.R. Burns [a], R.J.J. Jachuck [b,*]

[a] Process Intensification & Clean Technology (PICT) Group, Department of Chemical Engineering, Clarkson University, Potsdam, NY 13699, USA
[b] Protensive Ltd, Bioscience Centre, Centre for Life, Times Square Newcastle upon Tyne, NE1 4EP, UK

Received 2 June 2004

Abstract

Liquid–solid mass transfer performance on a 30 cm diameter spinning disc reactor is determined by use of the limiting current technique for copper deposition at different radial locations. Values for the local mass transfer coefficient are determined for a range of liquid flow rates and rotational speeds. The experimental data is compared with a model based on diffusion into a laminar flowing film and the enhancement in performance over this model is examined.
© 2005 Elsevier Ltd. All rights reserved.

Keywords: Thin film; Spinning disc reactor; Mass transfer; Diffusion; Limiting current

1. Introduction

The use of immobilized catalysts is an area of great interest for many chemical-manufacturing processes. Synthesis of chemicals using the batch-processing technique routinely use catalysts that are immobilized on the surface of fine particles in order to increase reaction surface area, mixing intensity whilst facilitating the speed of reaction. However such processes require the separation of the catalyst from the product by filtration and do not provide high shear between the reacting liquid and the solid catalyst surface. The mixing environment in such systems is strongly convective varying from location to location with modest heat transfer capabilities. This limits both the allowable and achievable reaction rates within such systems due to transport rate and selectivity constraints.

It has been realised however, that the concept of "Process Intensification" can offer alternative routes for these processes that alleviates some, if not all, of the constraints of the conventional batch process technology. The use of engineered mass transfer rates across well-defined diffusion path lengths is one alternative methodology to large scale convective "stirring". Microreactor technology utilises this concept by applying catalyst coatings to the walls of channels narrow enough to afford rapid mass transfer by diffusion alone [1]. However, in practice achieving such systems was a difficult process due to the inaccessible channel geometry and difficulty in re-sealing reactors if coatings were added whilst open. This led to innovative designs that used micro channels packed with immobilized particles, rather than coating the walls with the catalyst.

One alternative to the microchannel route is that of the spinning disc reactor (SDR) that is capable of generating

* Corresponding author. Tel.: +1 315 268 6325.
E-mail address: rjachuck@clarkson.edu (R.J.J. Jachuck).

0017-9310/$ - see front matter © 2005 Elsevier Ltd. All rights reserved.
doi:10.1016/j.ijheatmasstransfer.2004.11.029

Nomenclature

A	surface area for mass transfer, m^2
C_0	bulk concentration, mol m^{-3}
ΔC_1	concentration difference at entry, mol m^{-3}
ΔC_2	concentration difference at exit, mol m^{-3}
ΔC_{LM}	log mean concentration difference, mol m^{-3}
d	diameter of the cathode, m
D	diffusivity of the reactive ion, $m^2\ s^{-1}$
F	Faraday's constant defined as 96485 Coulomb per mole, C mol^{-1}
h	film thickness, m
I	current, A
k_{LS}	mass transfer coefficient, m s^{-1}
m_{Cu}	atomic mass, kg/kmol
n	electrons transferred per ion
N	mass flux per unit area, mol $m^{-2}\ s^{-1}$
N_A	average mass flux per unit area over a circular electrode, mol $m^{-2}\ s^{-1}$
Q	volumetric flow rate, $m^3\ s^{-1}$
r	radial co-ordinate, m
S	surface shear rate, s^{-1}
u_A	average velocity in the direction of flow, m s^{-1}
u_{dep}	deposition growth rate, m s^{-1}
w	width of the flow, m
x	distance in direction of flow, m
y	distance across the width of the flow, m
z	distance from the solid surface, m

Greek symbols

δ	diffusion layer thickness, m
v	kinematic viscosity of the liquid, $m^2\ s^{-1}$
ρ_{Cu}	density of pure copper, kg m^{-3}
ω	rotational speed of the disc, rad s^1

a film thickness typically as low as 10 μm through high centrifugal acceleration [2]. The ability to coat, activate and regenerate an exposed flat surface such as that of a spinning disc, though not trivial, is much less challenging than that of a confined channel. Combined with heat transfer capabilities typically of the order of 5–20 kW $m^{-2}\ K^{-1}$ [3,4] and rapid diffusive mass transfer, comparable to those of most microreactors, this should offer an ideal system for solid-catalysed liquid phase reactions.

In order to quantify the performance of a SDR for these processes it is essential to obtain the mass transfer coefficients between the liquid–solid interface. One common method that has been used to determine liquid–solid mass transfer coefficients is the "limiting current" technique. This technique has been described in several texts and is based on the measurement of the maximum achievable current through an electrode for a particular electrochemical process.

The work presented here describes how this measurement technique was adapted and used with a spinning disc reactor to obtain data on the liquid–solid mass transfer coefficients at different locations across the disc surface. The results are then compared with models based on diffusive transport to examine possible convective enhancements.

2. The limiting current technique

2.1. Relating current to mass transfer

The following section provides a summary of the limiting current method for determining liquid–solid mass transfer performance. This technique has been widely used in studies of liquid–solid mass transfer and in determination of diffusion coefficients. Several publications can be found discussing this subject, in particular Tobias et al. [5], Landau [6] and more substantively Selman and Tobias [7] and therefore only a brief description has been given here.

Direct current through a liquid is sustainable through an exchange of charge, in the form of electrons, between the ions and the electrode surface. This requires a driving potential to transfer the charge and to drive the ions through the fluid from electrode to electrode. The flow of electrons through the electrode can be related to the mass flux of the ions to the electrode through the following equation:

$$N = \frac{I}{A \cdot n \cdot F} \tag{1}$$

where F is the Faraday constant defined as 96485 Coulomb per mole and n is the electrons transferred per ion. This can be related to the liquid–solid mass transfer coefficient through the following equation:

$$k_{LS} = \frac{N}{\Delta C_{LM}} \tag{2}$$

where the log-mean concentration difference is defined as

$$\Delta C_{LM} = \frac{\Delta C_1 - \Delta C_2}{\ln(\Delta C_1 / \Delta C_2)} \tag{3}$$

where ΔC_1 and ΔC_2 are the concentration differences between the bulk and the surface at the start and end of the electrode. As the potential driving the current is

increased the concentration of the reacting species at the electrode are depleted until a point is reached at which all reactive ions reaching the surface are consumed. This generates an observed plateau, known as the "limiting current" in the process at which it can be assumed that the concentration of the ions at the surface is zero. At this point the values of ΔC_1 and ΔC_2 can be defined as

$$\Delta C_1 = C_0 \tag{4}$$

$$\Delta C_2 = C_0 - \frac{N \cdot A}{w \cdot h \cdot u_A} \tag{5}$$

where C_0 is the bulk ion concentration and the electrode is assumed to be rectangular of width w and area A with liquid film of thickness h flowing over with an average velocity u_A. As potential is increased beyond this plateau enough potential is generated at the electrode to drive other electrode reactions and current begins to increase. The point at which other reactions start limits the number of electrochemical processes that can be used for this technique to a few commonly used systems, one of these being copper deposition.

2.2. The copper deposition reaction

The process of cathodic copper deposition for the measurement of limiting current was chosen for these experiments. This was used primarily because of the ability to embed copper electrodes relatively easily into the surface of a spinning disc reactor and achieve a polished smooth finish. A second reason for this choice was that the copper produced a very low noise signal, in contrast to the use of stainless steel electrodes with a ferricyanide to ferrocyanide reaction, that is also commonly used and was considered for this work. Nickel electrodes which are superior to stainless steel electrodes were not considered due to fabrication difficulties. The negative aspect of this choice was the possible build up of deposits at the cathode interfering with the liquid flow. The scale of the deposition process was examined using the following equation for estimating the deposition growth rate:

$$u_{dep} = \frac{k_{LS} \cdot C_0 \cdot m_{Cu}}{\rho_{Cu}} \tag{6}$$

For this process the atomic mass of copper m_{Cu} is 63.55 kg/kmol and the density of copper ρ_{Cu} is 8920 kg m^{-3}. Assuming a typical mass transfer coefficient of 10^{-4} m s^{-1}, based on diffusion theory and later experimental observations, the deposition rate u_{dep} should be 1.5×10^{-9} m s^{-1} for the weak copper sulphate solution of 2.11 mol m^{-3} used in the experiments described here. This was four orders of magnitude smaller than the film thickness and was therefore assumed to be negligible for the duration of an experiment that was typically a few minutes.

3. Experimental facility

3.1. Construction of facility

The experimental facility was based on the same spinning disc reactor as described in the previous publication of Burns et al. [2]. A modified Perspex disc (PMMA) was used for these experiments. This was machined and embedded with 6 mm copper cathodes and a pair of long common copper anodes as shown in Figs. 1–3. Two sets of cathodes and anodes were used to balance the disc for rotation purposes. The anode was made with significantly greater area than the individual cathodes to ensure that the current was limited by the transport to the cathode. Wires were connected with screws in the base of the electrodes and relayed to the external circuit using a slip-ring assembly mounted at the base of the shaft.

The circuit used for the experiments is shown in Fig. 4. This was connected to a direct current power supply and two digital voltmeters. One voltmeter was used to measure the potential difference between the anode

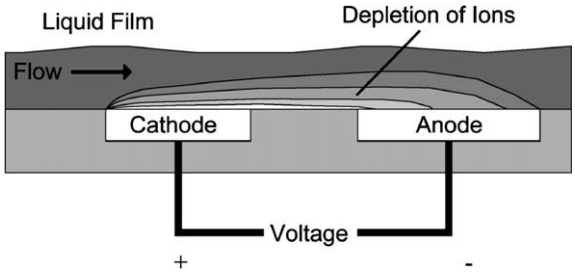

Fig. 1. Concept of the limiting current technique.

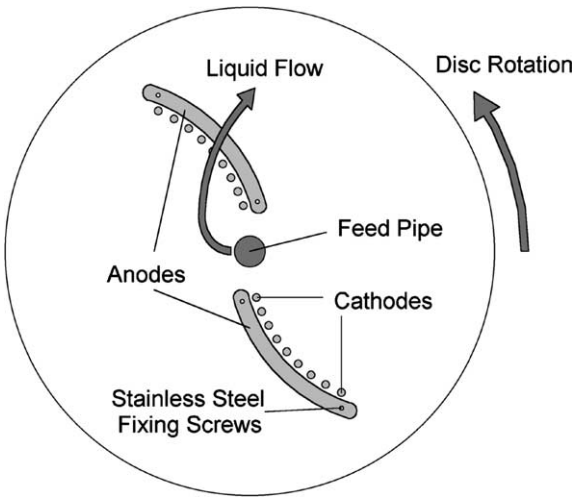

Fig. 2. Design of disc used for limiting current experiments.

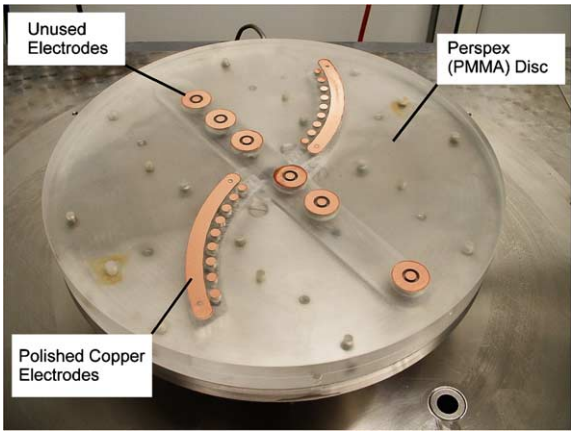

Fig. 3. Photograph of disc used for experiment.

and cathode and the other to measure the potential drop across a 1 kΩ load. The latter allowed the current through the electrodes to be calculated.

Several batches of liquids were tested on the system in the optimising of the measurement process. A summary of the final composition of the liquid used for all of the experiments documented here is given in Table 1. A solution containing 1 M of H_2SO_4 was required to provide a high enough conductivity through the thin film linking the electrodes. It also played a role in eliminating the transfer of Cu^{++} ions to the cathode surface by electrical migration. Even at this strength the procedure did require a significant driving potential to convey the current where the thinnest films were achieved. A relatively weak solution of copper sulphate was used to supply the copper ions for the process, this again was due to a combination of high mass transfer rates at the electrode surface and limitations on the conductance through the thin film linking them.

Table 1
Composition of the liquid batch used in the experiments

Specification	Quantity
Sulphuric acid (98%)	785 g
De-ionised water	7210 g
Copper sulphate ($CuSO_4$. $5H_2O$)	4.00 g
Batch volume	7.60 l
Batch density	1056 kg m^{-3}
Batch viscosity (at 20 °C)	1.24 mPa s
H_2SO_4 concentration	1.03 mol l^{-1}
$CuSO_4$ concentration	2.11 mol m^{-3}

The volume of liquid used in the batch was approximately 7.6 l. This was fed on to the disc using a centrifugal pump and flow was controlled with a needle valve. Flow was metered during the experiments using a small turbine flow meter located downstream from the needle valve. The liquid was injected onto the centre of the disc through a pipe with a 8 mm nozzle. The speed of the disc checked during experiments using a stroboscope.

3.2. Experimental procedure

At the start of each experiment the electrodes were polished using fine (1200 grade) emery paper to remove any roughness caused by copper deposition or depletion. The electrodes were then wiped over with a 1 M H_2SO_4 solution, dried and the system sealed. The disc rotation was set and liquid fed to the disc with the outflow being returned to the supply tank. Only one 6 mm diameter cathode was used in each experiment along with the adjacent anode. An initial potential of 0.2 V was set between the electrodes and left for 1 min. The voltage was then slowly increased whilst the potential across the

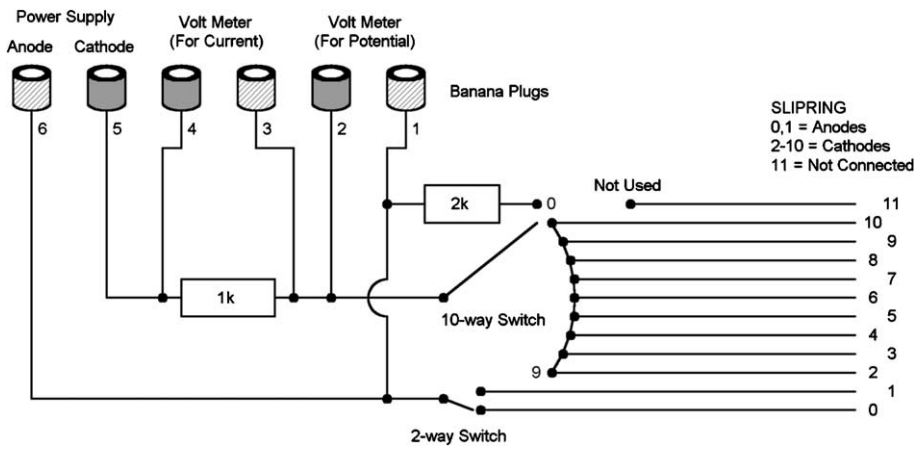

Fig. 4. Circuit used for measurement of current through electrodes.

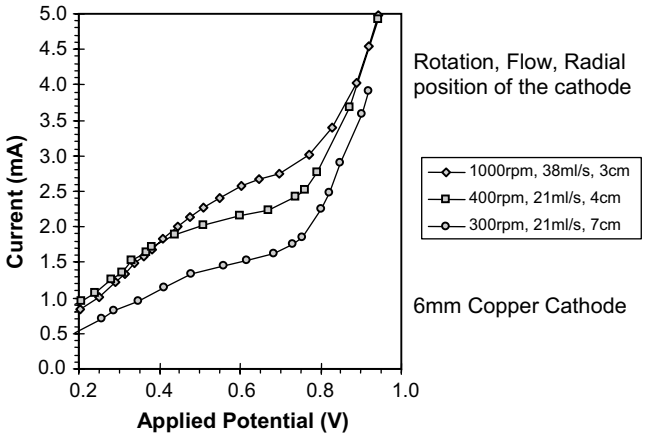

Fig. 5. Examples of limiting-current profiles obtained from the embedded electrodes.

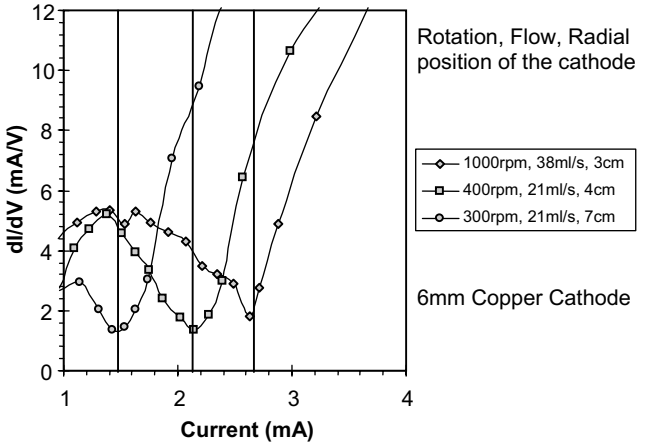

Fig. 6. The use of dI/dV gradient to highlight the limiting current. Examples shown using the same data as shown in Fig. 5.

electrodes and the current was noted at regular intervals. This was continued passed the limiting current, typically occurring in the region of 0.7 V, up to around 0.9 V. The profiles were then analysed using a spreadsheet.

3.3. Calculation of the limiting current

The limiting current is generally defined as the current at the point just prior to that at which the gradient begins increasing due to the start of the second reaction regime. Examples of the profiles obtained using this technique are shown in Fig. 5. Ideal profiles obtained for thicker films under non-rotating conditions showed a very clear limiting current plateau, however the experiments here often did not achieve such a distinct zone especially in cases of extremely thin films. Instead it was found that a point of inflexion, where the second reaction begins, was obtained. Unambiguous interpretation of this point was more easily achieved using a plot of dI/dV against current. An example of this is shown in Fig. 6. The limiting current for these experiments was therefore more clearly defined as the current at the point at which dI/dV is minimal, within a zone close to the second reaction starting. This is illustrated in Fig. 6 as the vertical lines.

It is acknowledged that the lack of a distinct long plateau for many results is not ideal for obtaining the high accuracy that this technique can achieve, however the results should provide a reasonable approximation for mass transfer calculations.

4. Calculation of mass transfer from the experimental data

Combining Eqs. (1) and (5) the effective concentration difference at the exit of the electrode can be calculated from the following equation.

$$\Delta C_2 = C_0\left(1 - \frac{I}{C_0 \cdot n \cdot Fd \cdot h \cdot u_A}\right) \tag{7}$$

where $n = 2$ for this process. The proportion of liquid flowing over the electrode of diameter d can be written as $(d/2\pi r)$. Replacing the volume flowing over the electrode, that is (dhu_A) with the proportion of the total flow, Eq. (7) can be re-written as

$$\Delta C_2 = C_0\left(1 - \frac{I}{C_0 \cdot n \cdot F \cdot Q} \cdot \frac{2\pi \cdot r}{d}\right) \tag{8}$$

For the experiments performed here the total flow was greater than 6 ml s^{-1}, the radial position of the electrodes was greater than 3 cm from the centre of the disc and the limiting current was less than 4 mA. Therefore a 6 mm electrode should deplete the feed concentration by less than 5%. Based on this estimate the log-mean concentration difference ΔC_{LM} was assumed to be equal to C_0 for the mass transfer analysis. Using this assumption and combining Eqs. (1) and (2) the liquid–solid mass transfer coefficient was estimated from the limiting current using,

$$k_{LS} \approx \frac{4I}{\pi d^2 \cdot n \cdot F \cdot C_0} \tag{9}$$

5. Experimental results

Experiments were performed using three liquid flow rates of 10, 21 and 38 ml s^{-1} and five rotational speeds of 200, 300, 400, 600 and 900 rpm. For each set of experimental conditions the limiting current was measured at nine radial positions, ranging from 3 cm to 11 cm at 1 cm intervals. This provided a total of 135 data points for analysis. Theoretical calculations for liquid–solid mass transfer performance based on laminar falling films Bird et al. [8] suggested that mass transfer coefficients should be strongly linked to local shear at the liquid–solid boundary.

In order to compare results against local shear for these experiments a model was required for the flow over the rotating disc. The simplest model for steady laminar falling film flow was provided by Nusselt [9] and assumes that viscous drag at the surface balances the weight of the falling film. A modified version of the Nusselt model is commonly used for flow over a rotating disc assuming that the liquid flow is synchronised with the disc rotation and under a similar force balance. Film thickness under this model is given by Burns et al. [2],

$$h = \left(\frac{3\nu Q}{2\pi r^2 \omega^2}\right)^{1/3} \tag{10}$$

Using Eq. (10) the average radial velocity u_A of the film can be written as

$$u_A = \frac{Q}{2\pi rh} = \left(\frac{1}{12\pi^2}\right)^{1/3}\left(\frac{Q^2\omega^2}{r\nu}\right)^{1/3} \tag{11}$$

Combining Eqs. (10) and (11) and assuming a parabolic velocity profile, surface shear S can be written as

$$S = \frac{3u_A}{h} = \left(\frac{3}{2\pi}\right)^{1/3}\left(\frac{Qr\omega^4}{\nu^2}\right)^{1/3} \tag{12}$$

Values of k_{LS} obtained from Eq. (9) were plotted against shear calculated from Eq. (12), using the values given in Table 2, with the results shown in Fig. 7. The results were also compared with predictions based on a falling film model provided by Bird et al. [8], the derivation of which is given in the next section.

The results shown in Fig. 7 indicate k_{LS} values in the range of 0.1–0.35 mm s^{-1} for an estimated shear rate of between 3000 s^{-1} and 50,000 s^{-1}. A significant scatter was observed in the results, however a general underlying trend of increasing mass transfer coefficient with shear was apparent. An improvement in performance at the lower flow rate of 10 ml s^{-1} was also apparent in comparison with the results at 21 and 38 ml s^{-1}. An exact reason for this was unclear and may be possibly due to inaccuracies in the flow model due to the spin-up zone or due to an artifact of the analysis technique.

A second common measure of mass transfer performance is that of the equivalent Nernst stagnant diffusion

Table 2
Values of constants used in calculations

Specification	Symbol	Quantity
Kinematic viscosity	ν	1.17×10^{6} m^2 s^{-1}
Cu^{2+} diffusivity	D	7.14×10^{-10} m^2 s^{-1}
Cu^{2+} concentration	C_0	2.11 mol m^{-3}
Cathode diameter	d	6×10^{-3} m

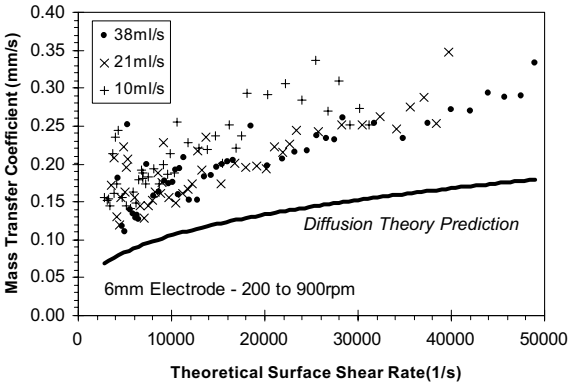

Fig. 7. Calculated mass transfer coefficients from experiments.

layer thickness δ as explained by Landau [6]. This can be defined in terms of the mass transfer coefficient k_{LS} as

$$\delta = \frac{D}{k_{LS}} \tag{13}$$

The diffusion layer thickness δ was computed for the experimental results and compared with the estimated film thickness given by Eq. (10). The results of this analysis are given in Fig. 8 and indicate a typical diffusion layer thickness over the 6 mm cathodes of between 2 μm and 6 μm compared with an estimated film thickness in the region of 50–250 μm.

6. Theoretical performance based on a laminar flow model

Mass transfer performance from the experiments was compared to that expected from simple diffusive transport. Given film thickness typically of the order of 10–100 μm and the flow velocity of the order of 0.1–1 m s^{-1} the Reynolds number for the flow should be typically in the region of 1–100 and laminar flow should therefore be a reasonable starting assumption. Assuming laminar flow over a plane surface the diffusion equation can be written as [10,8]

$$\frac{3}{2}u_A\frac{\partial C}{\partial x}\left(\frac{2z}{h}-\frac{z^2}{h^2}\right) = D\frac{\partial^2 C}{\partial z^2} \tag{14}$$

where the x-axis is parallel to the flow and the z-axis is perpendicular to the flow. A non-slip boundary condition is applied to the flow over the solid surface at $z = 0$. The average velocity of the film of thickness h is u_A. If the region of interest is assumed to be located close to the liquid–solid interface, as is the case for this work based on the results in shown in Fig. 8, the diffusion equation can be further approximated to

$$\frac{3z}{h}u_A\frac{\partial C}{\partial x} = D\frac{\partial^2 C}{\partial z^2} \tag{15}$$

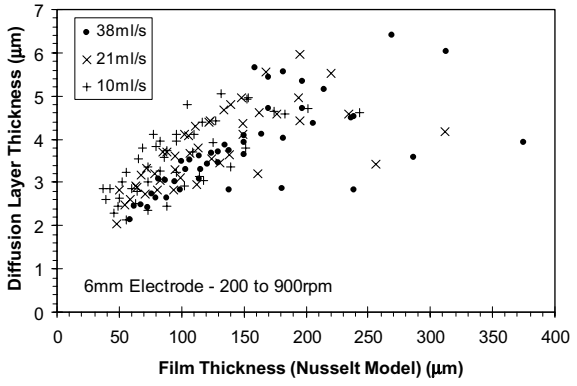

Fig. 8. Comparison of the diffusion layer thickness with the estimated film thickness predicted from the Nusselt flow model.

A solution of this equation can be reached through the following substitution:

$$\eta = z\left(\frac{S}{9Dx}\right)^{1/3} \tag{16}$$

where S is the shear rate at the liquid–solid interface that is defined for non-slip laminar flow as

$$S = \frac{3u_A}{h} \tag{17}$$

Bird et al. [8] provided details of the solution of Eq. (15) using this substitution and gives the average mass flux per unit area over a downstream distance L as

$$N = \frac{2DC_0}{\Gamma(7/3)}\left(\frac{S}{9DL}\right)^{1/3} \tag{18}$$

where

$$\Gamma(n) = \int_0^\infty \beta^{n-1}e^{-\beta}\,d\beta \tag{19}$$

Numerical integration of Eq. (19) gives $\Gamma(7/3) = 1.1906$. Inserting this value into Eq. (5) gives the average mass flux per unit area to be

$$N = 0.808.C_0\left(\frac{S\cdot D^2}{L}\right)^{1/3} \tag{20}$$

The expected mass rate through a circular electrode of diameter d, embedded in the solid surface, can be computed from Eq. (20) using the following integration:

$$\text{Rate} = \int_{-d/2}^{d/2} N\cdot(d^2-4y^2)^{1/2}\,dy \quad \text{where}$$
$$L = (d^2-4y^2)^{1/2} \tag{21}$$

where the length L is assumed to a chord through the circular area perpendicular to the line of integration that is across the diameter of the circle. Combining Eqs. (20) and (21) gives

$$\text{Rate} = 0.808\,C_0(S\cdot D^2)^{1/3}\cdot\int_{-d/2}^{d/2}(d^2-4y^2)^{1/3}\,dy \tag{22}$$

Substituting the dimensionless variable $y' = (y/d)$ into Eq. (9) gives

$$\text{Rate} = 0.808\,C_0(S\cdot D^2\cdot d^5)^{1/3}\cdot\int_{-1/2}^{1/2}(1-4y'^2)^{1/3}\,dy' \tag{23}$$

Solving numerically this gives

$$\text{Rate} = 0.680\,C_0(S\cdot D^2\cdot d^5)^{1/3} \tag{24}$$

This can be used to calculate an overall average mass flux per unit area N_A of

$$N_A = \frac{4\cdot\text{Rate}}{\pi d^2} \tag{25}$$

Combining Eqs. (25) and (2) provides a theoretical estimate for the mass transfer coefficient of

$$k_{LS} = 0.866\left(\frac{C_0}{\Delta C_{LM}}\right)\cdot\left(\frac{S\cdot D^2}{d}\right)^{1/3} \quad (26)$$

Application of this model to the flow over the rotating disc can then be made by substituting the estimated value of surface shear given in Eq. (12) into Eq. (26). This gives

$$k_{LS} = 0.798\left(\frac{C_0}{\Delta C_{LM}}\right)\cdot\left(\frac{Qr\omega^4 D^6}{\nu^2 d^3}\right)^{1/9} \quad (27)$$

Using the values given in Table 2 for this system a curve for the estimated mass transfer coefficient based on Eq. (27) was shown in Fig. 7 assuming $\Delta C_{LM} = C_0$. It was observed that the results were higher than this prediction by a factor of between 1.3 and 3.0 with an average enhancement factor of 1.8 over the 135 data points.

It is unclear from the scope of this study where enhancements over diffusive transport, as indicated in the results of Fig. 7, may lie. One possibility could include convection due to surface waves that has been suggested in earlier work with SDRs [3,4]. However it is unclear how deep the phenomena can reach and has been mainly studied for gas–liquid processes. Another possible phenomena could be a breakdown in the non-slip boundary condition that could lead to enhanced transport compared to the model. It could also simply be due to an inaccuracy in the Nusselt model assumed here. The latter possibility can be examined through the work of Burns et al. [2] that indicates significant tangential shear within the spin-up zone. However this influence would fade towards the periphery especially for lower flow rates and this is not indicated in the results of Fig. 7. It cannot of course be ruled out that surface roughness could enhance the performance, although care was taken to polish the electrodes between each experiment.

7. Conclusions

The limiting current described here has provided an insight into the mass transfer performance of spinning disc reactors at the liquid–solid interface. The technique has been stretched due to the thinness of the film and the results given may therefore not be as accurate as normally achievable from this technique. However as the results were based on the current achieved before the second reaction, they must provide an accurate minimum for the calculation of k_{LS}. This would imply that liquid–solid mass transfer coefficients for a spinning disc reactor (SDR) can be expected to be of the order of 10^{-4} m s^{-1}. Combined with the thin film of the order of 10^{-4} m this should provide excellent mass transfer performance for chemical processing over time scales of the order of a second.

Comparison with diffusion theory has also shown that the results are of a similar order to that expected for laminar flow over the disc and again are above that predicted from the model. This would imply that the models given in Eqs. (10), (11) and (14) should provide a good basis for predicting the minimum mass transfer performance for SDRs.

Acknowledgement

The authors would like to thank EPSRC, UK for providing funding for this activity under the IMI programme.

References

[1] W. Ehrfeld, V. Hessel, L. Holger, Microreactors: New Technology for Modern Chemistry, WILEY-VCH Federal Republic of Germany, 2000.
[2] J.R. Burns, C. Ramshaw, R.J.J. Jachuck, Measurement of liquid film thickness and the determination of spin-up radius on a rotating disc using an electrical resistance technique, Chem. Eng. Sci. 58 (11) (2003) 2245–2253.
[3] R.J.J. Jachuck, C. Ramshaw, Process intensification—heat transfer characteristics of tailored rotating surfaces, Heat Recovery Syst. CHP 14 (5) (1994) 475–491.
[4] A. Auone, C. Ramshaw, Process intensification: heat and mass transfer characteristics of liquid films on rotating discs, Int. J. Heat Mass Transfer 42 (1999) 2543–2556.
[5] C.W. Tabias, M. Eisenberg, C.R. Wilke, Diffusion and convection in electrolysis—a theoretical review, J. Electrochem. Soc. 99 (12) (1952) C359–C365.
[6] U. Landau, Determination of laminar and turbulent mass transport rates in flow cells by the limiting current technique, AIChE Sympos. Ser. 77 (204) (1981) 75–87.
[7] J.R. Selman, C.W. Tobias, Mass transfer measurements by the limiting current technique, Adv. Chem. Eng. 10 (1978) 211–318.
[8] R.B. Bird, W.E. Stewart, E.N. Lightfoot, Transport Phenomena, Wiley, New York and London, 1960, pp. 551–552.
[9] W. Nusselt, Die Oberflächenkondensation des Wasserdampfes, Z. Ver. Deut. Ing. 60 (1916) 541.
[10] J. Crank, The Mathematics of Diffusion, second ed., Clarendon Press, Oxford, 1975, pp. 44–68.